THE UNIVERSITY of EDINBURGH

Edinburgh Research Explorer

Ring closing reaction in diarylethene captured by femtosecond electron crystallography

OPEN ACCESS

Ring-Closing Reaction in Diarylethene Captured by Femtosecond Electron Crystallography**

Hubert Jean-Ruel,[1,2] Meng Gao ,[1,2] Michal A. Kochman,[3] Cheng Lu,[1] Lai Chung Liu,[1,2] Ryan R. Cooney,[1] Carole A. Morrison[3] and R. J. Dwayne Miller[1,2,*]

[1]Departments of Chemistry and Physics, University of Toronto, 80 St. George Street, Toronto, Ontario M5S 3H6, Canada

[2]Max Planck Institute for the Structure and Dynamics of Matter, Luruper Chaussee 149, Hamburg 22761, Germany.

[3]EaStCHEM, School of Chemistry, Joseph Black Building, University of Edinburgh, West Mains Road, Edinburgh, EH9 3JJ, UK.

[*]Corresponding author; e-mail: dwayne.miller@mpsd.cfel.de; tel: +49 (0) 40 8998 6200

Supporting information:
Additional details on the experiment, analysis, and theoretical calculations are provided. The first section gives more information on the data acquisition and averaging. The second section describes the determination of the crystal orientations. Figure S1 shows an example of diffraction image processing and Figure S2 presents the orientation match. The third section details the determination of the theoretical t∞ differential images. Figure S3 compares the simulated differential images

obtained using the absolute intensity changes with those obtained using the relative intensity changes. The fourth section presents the model analysis. Figure S4 presents the 4 basic motions considered, Figure S5 demonstrates that their application to the open-ring geometry results in the closed-ring one, and Figure S6 shows the range of structures that they generate. Figure S7 compares the best matching structure for the time delays before t0 with the one for the late time delays. The fifth section presents the details of the calculation of the ground state structures. The optimized geometries of the four molecules included in the unit cell are shown in Figure S8, first (a) with all four in the open-ring state, and then (b) after inducing the cyclization in one of them. Finally, the sixth section presents the details of the calculation of the excited state open-ring intermediate structure. Figure S9 shows the partitioning of the system into CASSCF and DFT regions and Figure S10 shows the optimized geometry. This material is available free of charge via the Internet at http://pubs.acs.org

Graphical abstract:
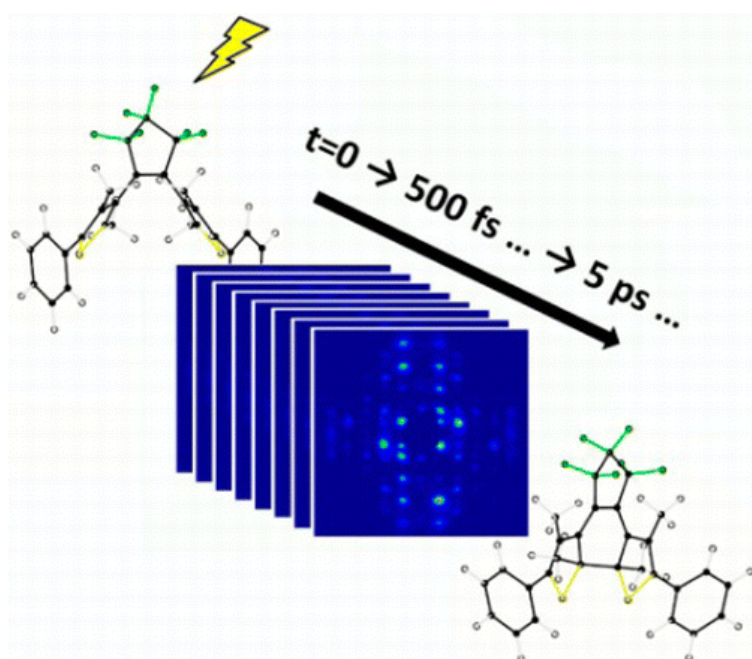
Abstract:
The photoinduced ring-closing reaction in diarylethene, which serves as a model system for understanding reactive crossings through conical intersections, was directly observed with atomic resolution using femtosecond electron diffraction. Complementary ab initio calculations were also performed. Immediately following photoexcitation, subpicosecond structural changes associated with the formation of an open-ring excited-state intermediate were resolved. The key motion is the rotation of the thiophene rings, which significantly decreases the distance between the reactive carbon atoms prior to ring closing. Subsequently, on the few picosecond time scale, localized torsional motions of the carbon atoms lead to the formation of the closed-ring photoproduct. These direct observations of the molecular motions driving an organic chemical reaction were only made possible through the development of an ultrabright electron source to capture the atomic motions within the limited number of sampling frames and the low data acquisition rate dictated by the intrinsically poor thermal conductivity and limited photoreversibility of organic materials.

I. Introduction

Directly resolving the atomic motions involved in various physical, chemical, and biological processes has been achieved through the recent development of ultrabright and ultrafast electron and X-ray sources[1-3]. The strategy consists of exciting the system under study with fs laser pulses and probing its structure via diffraction with synchronized ultrashort electron or X-ray bunches; by varying the time delay between the laser and probe pulses, the recorded diffraction patterns monitor the structural changes. The first studies that attained sufficient diffraction orders to atomically resolved structural dynamics on the relevant time scales focused on relatively simple condensed-phase systems with well defined changes in order parameters[4-10]. The challenge has been to extend this approach to labile and weakly scattering organic and biological systems in which the structure changes are more complex. Various photoinduced processes in organic crystals have been investigated with time-resolved X-ray diffraction, but so far the limited time resolution (probe pulses on the order of 50 ps or longer) has generally prevented the direct observation of the primary structural dynamics occurring on subpicosecond time scales[11-14]. More recently however, the molecular motions involved in the insulator-to-metal phase transition of a charge-transfer organic system, $(EDO-TTF)_2PF_6$, were successfully resolved with fs resolution using ultrafast electron diffraction (UED)[15]. The structural changes in this organic system were driven by a photoinduced charge transfer process. Nevertheless, despite the numerous successes of ultrafast diffraction techniques, the direct observation of the structural changes relevant to understanding chemical reaction mechanisms, as opposed to phase transitions, has not been achieved to date with sufficient time resolution to resolve the key dynamics involved. This work takes advantage of the recent advance in electron source brightness to directly observe the atomic motions driving reaction dynamics. This new window

on chemistry will allow general principles to be established in understanding how far from equilibrium fluctuations couple during barrier crossing events that lead to an enormous reduction in dimensionality and ultimately make chemical reaction concepts transferrable from one molecular system to another.

Of particular interest are *solid state* organic photochemical reactions. Although great efforts have been deployed towards gas phase diffraction studies[16-18], the time resolution attained to date is insufficient (several ps) to capture the relevant motions, and the level of detail with respect to spatial resolution achievable with time-resolved crystallography is incomparable. Moreover, the dynamics are generally better defined in the crystalline state due to the homogeneous intermolecular potential[14, 19]. There are, nevertheless, important challenges with performing ultrafast diffraction studies of solid state organic photochemical reactions. The vast majority of molecular crystals are insulators and they usually have low melting points. The consequence is that low repetition rates must be used to avoid cumulative heating effects that induce both crystal strain and artifacts in the dynamics. More importantly, chemical reactions taking place in the crystalline state are generally irreversible or exhibit a limited number of photo-excitation cycles[20]. All these characteristics impose strong conditions on the source brightness.

A notable example of a solid state organic photochemical reaction occurs in certain diarylethene compounds. Diarylethenes with heterocyclic aryl rings are a family of photochromic molecules which undergo photoinduced ring closing (cyclization) and ring opening (cycloreversion) of the molecular system in both solution and the crystalline phase[21]. Photochromism refers to their ability to undergo such photoreversible isomerization between two

isomers with different absorption spectra. This property, together with their capacity to undergo a large number of cyclization and cycloreversion cycles before significant degradation, make them good candidates for optoelectronic applications such as all-optical memories and switches[21, 22]. For this reason, and also because of the potential application of certain derivatives in their crystalline state to act as light-driven nano- and microactuators[23-25], diarylethenes with heterocyclic aryl rings have been the subject of recent extensive study.

The ring closing reaction in photochromic diarylethene also represents a textbook example of classic electrocyclic reactions. A large number of time-resolved spectroscopic and theoretical studies have been performed on these systems, revealing that the cyclization reaction occurs on sub-ps to ps time scales[19, 26-39] and proceeds through the crossing of a conical intersection[40-42]. To understand the mechanism of ring closing, we need to know the specific motions that direct the system through the barrier cross region or define the conical intersection between the ring-open and -closed electronic surfaces. It is these motions that define the reaction saddle point and effective barrier height. This information is critical to controlling the chemistry of interest.   In this regard, all-optical measurements are only indirectly sensitive to the structural changes associated with the reaction and cannot provide a complete atomistic description that is needed to understand the chemistry at the most basic level.

Here we present UED measurements of the ring closing reaction in the single crystal diarylethene derivative 1,2-bis(2,4-dimethyl-5-phenyl-3-thienyl)perfluorocyclopentene (Scheme 1), performed with our recently developed ultrabright fs electron source[43]. Complementary *ab*

initio calculations are also presented in order to assist the time-resolved crystallography measurements.
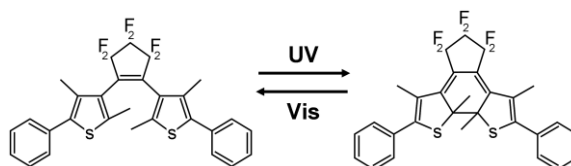
Scheme 1

The general considerations and constraints discussed above for solid state organic chemical reactions fully apply to this study. Furthermore, the thermal irreversibility of the isomerization reactions in diarylethene represents an additional experimental difficulty. Following every cyclization pump-probe event, cycloreversion must be photoinduced with a second laser beam to bring the crystal back to its fully open-ring state, further reducing the repetition rate achievable. However, this property also confers two very important advantages over thermally reversible reactions. First, the thermal stability of the system can be exploited to systematically compare the time-resolved diffraction signal with that of the final product and thus to explicitly monitor the convergence to the ring-closed structure. Second, we can be confident from the well defined photoproduct diffraction when the sample is in the photoreversible regime, independent from the time-resolved signal, which is extremely important to prevent strain-induced effects from biasing the findings.

This study is the first to directly probe the structural changes involved in a solid state organic chemical reaction with sub-ps resolution. It paves the way for the use of UED to determine the key atomic motions involved in complex organic systems. The complementary quantum mechanical calculations also represent a great advance with respect to determining structural

minima on excited state potential energy surfaces in the crystalline phase and in the vicinity of conical intersections. The theory greatly complements the experimental studies and analysis, to provide further checks and constraints for extracting the key motions from the diffraction data.

II. Experimental and Computational Methods

Powdered 1,2-bis(2,4-dimethyl-5-phenyl-3-thienyl)perfluorocyclopentene (Tokyo Chemical Industrial Co.) was dissolved in hexane (5 g/L) and single crystals were grown in the dark by slow solvent evaporation. The crystals were microtomed to 100-150 nm thickness and mounted on standard TEM copper meshes covered with lacey Formvar. Different orientations were obtained by microtoming the single crystals along different planes.

The UED measurements were conducted in transmission mode with a recently developed ultrabright source consisting of a 95 kV DC photoelectron gun in combination with a radio frequency rebunching cavity (details of the system are presented elsewhere[43]). The pump and electron probe pulses were both derived from the frequency tripled (270 nm) output of a Ti:sapphire oscillator (Coherent Micra) and associated regenerative amplifier system (pulses at 810 nm, 50 fs, and 500 μJ). The electron probe pulses were generated by photoemission from a gold photocathode, followed by subsequent acceleration at 95 keV and compression by a 3 GHz RF cavity. Pulses of 70 fC were used. The UED system has an overall temporal instrument response function of 430 fs, with sufficient stability and signal to noise to extract 100 fs structural dynamics[43]. To induce ring closing, the pump fluence was set to 0.35 mJ/cm^2 at the sample position and the pulses were stretched to approximately 300 fs in order to minimize the peak power to avoid multiphoton ionization artifacts. Only a small fraction of the molecules

were converted to the closed-ring form at each cycle. Following each UV pump pulse, a cw HeNe laser (633 nm, 2 mW) irradiated the sample for 10 seconds to convert all the molecules back to their initial open-ring state. It should be emphasized that the overall repetition rate was thus limited to approximately 0.1 Hz, which is 4 orders of magnitude slower than the majority of UED experiments which are performed at 1 kHz. This low repetition rate also ensured the absence of any accumulated heating effect on the dynamics of interest. The electron probe, UV pump, and HeNe beam spot sizes at the sample position were respectively 400 μm, 600 μm, and 700 μm. To perform the time-resolved measurements, the pump pulses impinge on a variable delay stage in order to systematically vary the path length of the pump relative to the probe to measure the temporal dependence of the photoinduced changes in diffraction intensity.

Throughout the data collection, independent determination of t_0 – which is subject to drift with the RF compression technique and can compromise the time resolution– was performed once every hour in between scans using the previously described method of photoelectron bunches deflection from laser induced surface plasma on a copper mesh[44]. For the t_0 correction, a 810 nm pulse, collinear and matched in time with the 270 nm pump employed for the UED measurements, was used to generate the plasma.

For each pump-probe event, three distinct diffraction patterns were acquired prior to photo-inducing the cycloreversion: *before* (pump-off), *during* (pump-on), and *after* (pump-off, before cycloreversion). The difference in diffraction intensity between the *during* and *before* images corresponds to the time-resolved signal, while the difference intensity between the *after* and the

before images corresponds to the t_∞ signal, effectively the difference between equilibrium closed ring and open ring patterns.

The indexing and orientation determination of the fully open-ring experimental electron diffraction patterns were performed with the help of a simulation program developed in-house, which has been reported previously[15]. The structure obtained previously by X-ray diffraction[23] is considered. The observed diffraction patterns were well reproduced by the simulations, the resulting R factors varying between 0.23 and 0.34 (see Supporting Information). To simulate the diffraction patterns of the closed-ring form (and of the model structures), since only a fraction of the molecules are converted during each cycle, the structure factors of both the open- and the closed-ring (or model) structures were combined according to a simple method presented previously for time-resolved crystallography analysis[45]. The method considers a random distribution of excited (or converted) molecules in the initially fully open-ring crystal. Such photo-induced disorder results generally in a reduction of the average diffraction intensity, but the specific behavior of the individual peaks – i.e. to increase or decrease in intensity by a given magnitude – depends on the actual molecular structural changes of the excited (or converted) molecules[46].

The open-ring electronically-excited intermediate was optimized on a potential energy surface using the QM/QM paradigm[47], whereby the reactive molecule is treated using the CASSCF method with a localised basis set, while the surrounding crystal lattice is described on the DFT level with a plane-wave basis set. The bulk lattice surrounding the photoexcited molecule was described using the PBE exchange-correlation functional[48] as implemented in the software

package CASTEP version 5.0[49]. A plane-wave cutoff of 400 eV was applied. The electronic Brillouin zone was sampled at the (0 1/4 0)-point only. The default ultrasoft pseudopotentials were used[50], and energies and forces were corrected for dispersion interactions using the semiempirical scheme of Grimme[51]. The same level of DFT theory was applied in the optimizations of the ground-state open- and closed-ring structures, except that the plane-wave cutoff was increased to 500 eV. The photoexcited state of the reactive diarylethene molecule was treated at the state-specific CASSCF level, as implemented in the software package GAUSSIAN09[52]. According to the previous CASSCF study on the photocyclization reactions of diarylethenes[42], an active space consisting of 10 π and π^*-type orbitals provides a realistic description of the potential energy surface of the open-ring isomer. Therefore an active space consisting of 10 canonical π and π^*-type orbitals, which were mostly localized on the thiophene rings, was used in all CASSCF calculations reported in the present work. Note due to computational costs the pendant benzene rings have been omitted from the CASSCF calculations, and the resultant dangling valency sites on the thiophene rings capped with hydrogen atoms. As a compromise between computational cost and tractability, the 3-21G basis was applied in the CASSCF calculation, corresponding to a quality similar to that used in the aforementioned theoretical study on free diarylethene molecules[42].

III. Results and Discussion

3.1 Static electron diffraction measurements and comparison with ground state calculations.
The reversibility of the structural changes associated with cyclization and cycloreversion of a fraction of the molecules in crystalline diarylethene was investigated with static electron diffraction, subsequent to each photocycle step. Concurrently, the sensitivity of

the diffraction patterns produced by various crystal orientations to the atomic motions involved was also assessed. Figure 1a-c show the electron diffraction patterns of the crystal in its initially open-ring state for three distinct orientations. Figure 1d-f show the corresponding differential images – the difference between the diffraction patterns of the open- and closed- ring states – following the ring closing of a fraction of the molecules by single fs UV pulses. It can be observed that several Bragg peaks exhibit a significant change in diffraction intensity, demonstrating our capability to probe the relevant structural changes involved in the ring closing reaction. It must be emphasized that the signals observed in Figure 1d-f correspond effectively to the t_∞ point in a time-resolved experiment.
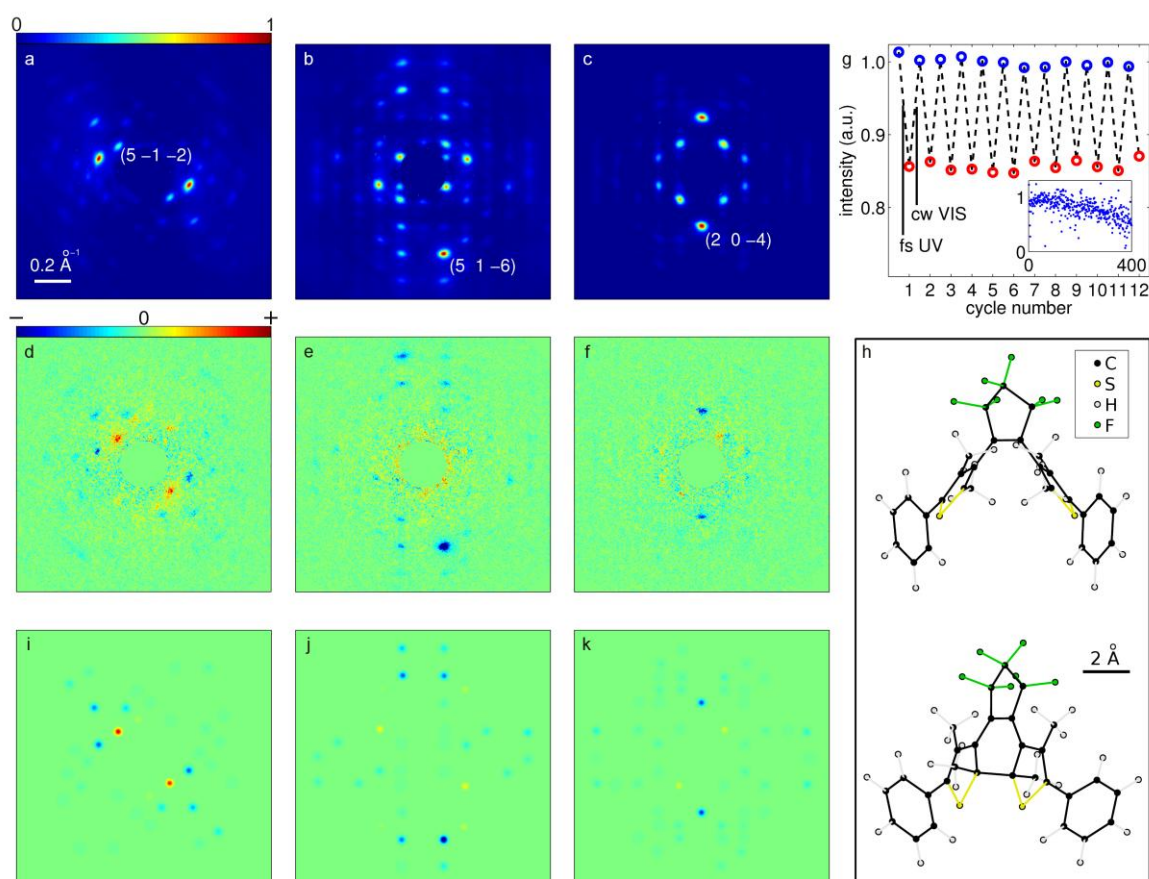
Figure 1. Static electron diffraction measurements and comparison with ground state calculations. (a-c) Diffraction patterns of the fully open-ring form for the crystal orientations [0.45 0.19 0.87], [-0.77 0.17 -0.62], and [0.87 -0.02 0.49]. Each image corresponds to the average of 5-10 different samples. The assigned Miller indices are displayed for selected peaks. (d-f) Differential intensity changes associated with the patterns presented in (a-c) following photoinduced ring closing induced by single UV excitation pulses. (g) Normalized intensity of the reflection (5 1 -6) for the first 12 cyclization and cycloreversion cycles, induced respectively with single UV pulses and cw visible light. The inset shows the normalized absolute intensity change for the first 400 cycles. (h) Starting open-ring and closed-ring photoproduct geometries optimized in the open-ring crystal lattice at the DFT level of theory. (i-k) Simulated differential intensity changes based on the calculated structures.

   Figure 1g reports the normalized diffraction intensity of the Bragg peak (5 1 -6) as a sample is cycled between the open- and closed-ring states, following subsequent irradiation by single UV pulses and continuous wave (cw) visible light. It can be observed that the change in diffraction intensity is both reversible and repeatable. Similar results were obtained for all Bragg peaks exhibiting an intensity change. This confirms the reversibility of the structural changes with the excitation conditions used, which allows pump-probe measurements to be performed without constant exchange or translation of sample. The inset presents the normalized absolute difference in diffraction intensity of the same Bragg peak for 400 cycles. It can be observed that approximately 300 repeatable cycles are achieved, considering a 70% criterion. This result is typical; depending on the sample, the number of photocycles available for the time-resolved experiment varied between 100 and 500 cycles. This limited repeatability represents a major

challenge for performing time-resolved crystallography measurements. However, it remains feasible to achieve the signal-to-noise ratio (SNR) required to accurately follow the structural changes of interest due to the high reproducibility of the samples, the consistency of the UED system, and its single-shot diffraction pattern acquisition capability even in the sub-ps resolution regime.

In order to further confirm that the observed changes in diffraction intensity result directly from the structural changes associated with the ring closing reaction, the theoretical difference intensities were determined using the calculated open- and closed-ring ground state structures in the open-ring crystal lattice. The latter geometries, optimized at the DFT level of theory, are presented in Figure 1h. Figure 1i-k show the resulting simulated differential images for the three crystal orientations presented above, considering a conversion of 2.9 % of the molecules from the open to the closed-ring calculated structures. It can be observed that the general agreement is excellent with the corresponding experimental results presented in Figure 1d-f. Considering the reliable high intensity peaks (22), the Pearson correlation coefficient for the relative intensity changes is 0.87. The strong correspondence between the experimental and simulated changes in diffraction intensity fully confirms that the structural changes associated with the ring closing reaction are appropriately probed. (See Supporting Information for details on the theoretical differential images, the correlation calculation, and the structures optimization.)

3.2 Time-resolved electron diffraction measurements. UED measurements were performed to determine the temporal evolution of the diffraction intensity of the various Bragg peaks in order to follow the formation of the closed-ring photoproduct. Three main trends were observed

and are explained below. Representative results are presented in Figure 2. The relative change in diffraction intensity is given as a function of the time delay between the fs electron probe pulses and the fs UV pump pulses. As mentioned previously, the t_∞ point was systematically measured after every pump-probe event and is equivalent to the difference intensities displayed in Figure 1d-f. Monoexponential fits with constant offset are shown in Figure 2a-b, with time constants of $\tau = 3$ and $\tau = 5$ ps respectively.
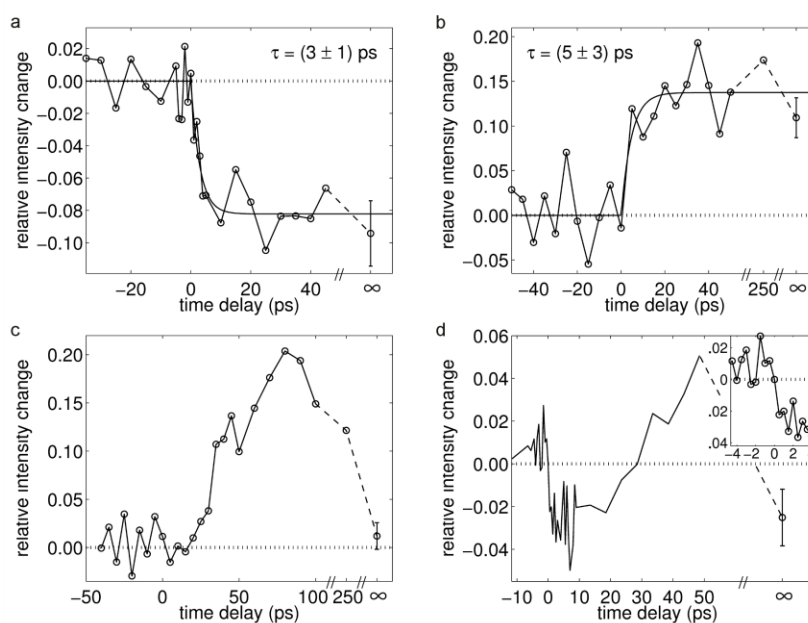
Figure 2. Time-resolved relative changes in diffraction intensity following photoexcitation for selected reflections. (a-d) Dynamics of Bragg peaks (5 1 -6), (5 -1 -2), (2 0 -2), and (2 0 -4) respectively, averaged from a total of 18 samples. The error on the t_∞ point corresponds to the standard deviation of the measured values within the crystals considered. The error on the time-resolved data (all time points except t_∞) can be estimated from the noise before t_0. Dashed rather than solid lines are used to link the last time points to highlight the change of time scale. Exponential fits with constant offset are displayed in (a) and (b). Although bi-exponential

dynamics are expected for this system, mono-exponential fits were performed because of the limited SNR.

The signals presented in Figure 2a-b are typical and a similar behaviour was observed for several other Bragg peaks. A change in diffraction intensity is developed with a time constant of a few ps and the signal amplitude for the time points beyond 20 ps is approximately equal to the t_∞ signal. Since it was unambiguously established in the previous section that the changes in diffraction intensity observed at t_∞ correspond to the cyclization of a fraction of the molecules, the UED signals shown in Figure 2a-b are directly attributed to the structural changes involved in the ring closing reaction. Furthermore, the observed time scale agrees with the results of the transient absorption measurements reported previously on the same compound also in the crystalline state[19]. Time constants of 200 fs and 5.3 ps were found for the formation of the open-ring excited state intermediate and of the closed-ring molecule, respectively, both of which involve structural changes. Bragg planes for which the dominant contribution to the dynamics is the ring closing step should exhibit a time constant on the order of 5 ps or slightly less, which corresponds to what is observed in Figure 2a-b. The successful probing of the photoproduct formation and the direct confirmation of its time-scale constitute a key result of this study.

The signal presented in Figure 2c was also observed for a number of Bragg peaks. It consists of a slow signal of generally large amplitude, exhibiting a rise time on the order of 80 ps, and for which the late time points are not equal to the t_∞ signal. Such behaviour is not reflective of permanent structural changes. Instead, it is indicative of strain waves, which result from the stress induced in the crystal film following the ring closing of a fraction of the molecules within

the open-ring crystal lattice. Similar strain signals were reported in other UED studies[15, 53]. Nevertheless, only a minority of Bragg peaks exhibited strain signals, and since they are easily identifiable as signal modulation and are well separated in time, they did not influence the monitoring of the ring closing reaction. Keeping 18 of the 22 peaks considered above (i.e. those free of strain signal to further reduce any influence on the analysis), the Pearson correlation coefficient between the average relative diffraction intensity changes measured between 10 and 50 ps and the ones simulated from the calculated closed-ring state is 0.92.

Finally, the signal presented in Figure 2d exhibits a clear sub-ps decrease in diffraction intensity (followed by a strain signal), confirming the existence of an intermediate structure formed on this time scale. This constitutes another key result of the study. More specifically, the ultrafast signal is attributed to the initial evolution of the open-ring molecules on the excited state potential energy surface prior to ring closing. The behaviour of the UED signals implies that the formation of the intermediate state brings the initially open-ring molecules towards the closed-ring structure, while being clearly distinct from the latter. This follows from the fact that the different Bragg peaks exhibit relatively smooth intensity changes towards the ring-closed level (no extravagant behaviour was observed near t=0), but they do so at different rates.

At this point, it is important to emphasize the significant advance of this work with respect to the UED measurements that we reported previously to complement a spectroscopic study on the same system[19]. In the latter, we demonstrated the feasibility of this experiment and resolved the change in diffraction intensity of one Bragg peak with 10 ps time steps. In the current study, we resolved the UED signal associated to a large number of diffraction peaks, from several crystal

orientations, and we improved by more than one order of magnitude the time resolution due to the advancement of our ultrabright electron source. The number of diffraction orders and time resolution is now sufficient in principle to unambiguously distinguish between different possible motions leading the system to the conical intersection on the excited state surface, as limited in practice only by the SNR. Furthermore, we present here a comprehensive analysis which includes notably the unambiguous assignment of the t_∞ diffraction changes to the ring closing reaction, providing a clear interpretation for the associated UED signals observed. The quality and time resolution of the present diffraction data, together with theoretical calculations, enables reconstruction of the key motions directing the ring closing reaction.

3.3 Model analysis and intermediate structure calculation. To gain more insights on the intermediate structure, and also to further confirm the convergence of the diffraction patterns towards the closed-ring molecule, a simple model was constructed in order to generate a pool of molecular structures to compare with the time-resolved data. It was found by inspection that a small number of basic rotations – four pairs consisting of seven pure rotations and one torsion – could convert the open-ring structure presented in Figure 1h into the closed-ring one (details of the model analysis are given in Supporting Information). The different motions were allowed to vary independently. The average changes in diffraction intensity for time delays between 10 and 50 ps were compared to the ones generated by the model structures. The average of the top 1% best matching structures is presented in Figure 3a. It is similar qualitatively to the calculated product geometry shown in Figure 1h.

The amount of reliable experimental data available to investigate the intermediate structure is limited by the SNR for the various diffraction orders. Nevertheless, the changes in diffraction intensity of the strongest reflections immediately following photoexcitation were compared to those generated by the model structures in order to identify a possible trend with respect to the key motions involved. It was found that the best matching structures are those for which the thiophene rings are significantly rotated while the perfluorocyclopentene ring is only slightly rotated, as shown in Figure 3b. Higher SNR would be required to precisely extract the intermediate state structure. Nevertheless, we believe this relatively simple method of analysis could prove to be of general importance in extracting structural information from FED measurements of complex organic reactions.
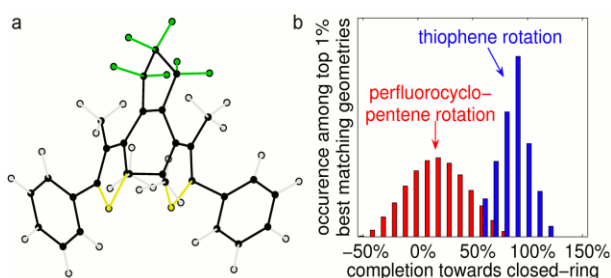
Figure 3. Model analysis of the UED data. (a) Experimental photoproduct: best matching model structure for the time delays between 10 and 50 ps. The 18 most reliable reflections were included (Bragg peaks with large diffraction intensity – above 35% of maximum intensity – and which exhibit no strain waves). The top 1% matching structures were averaged together to obtain a representative result of the overall convergence. (b) Experimental intermediate: distribution of the percentage completion (with respect to the closed-ring geometry) of the thiophene and perfluorocyclopentene rotations among the top 1% matching structures for the time delays

between 0.5 and 3 ps. Because of the significantly lower SNR, only the 9 strongest reflections – above 65% of maximum intensity – from the two orientations which were measured with short time steps were included.

In order to provide a clearer picture of the excited-state open-ring intermediate structure, an *ab initio* theoretical model was constructed using the QM/QM paradigm, which we have described in full elsewhere[47]. The output from this calculation corresponds to the fully-optimised intermediate structure labelled HT* (in accordance with the labelling scheme of Boggio-Pasqua *et al*.[42] presented in Figure 4) embedded in a crystal lattice of fully-optimised electronic ground state molecules. The structure of this ring-open intermediate is very similar to that proposed theoretically for a free molecule by Boggio-Pasqua *et al.*, with a shortened distance of 2.19 Å between the two reactive carbon atoms (c.f. 3.71 Å in the fully ring-open state HT, and 1.56 Å in the fully ring-closed state CHD). The optimized structure is presented in Figure 5, overlaid on the open-ring molecule. The main structural change is a significant rotation of the thiophene rings which acts to flatten the molecule considerably. In contrast, the rotations of the benzene and perfluorocyclopentene rings are very small (see Supporting Information for details). Thus, most of the structural change appears to involve the thiophene rings, with minimal motion observed for the perfluorocyclopentene moieties. This finding is in qualitative agreement with the noted behaviour based on the above analysis of the experimental results. That said, the fact that the pendant benzene rings were omitted from the CASSCF calculations is a potential source of weakness and will require further theoretical investigation. Moreover, whether the intermediate state captured in the UED experiment is directly the HT* structure, or corresponds

to a mixture composed of the HT* intermediate and some other state, perhaps involving the conical intersections CI4 or CI5 (see Figure 4), will require further theoretical investigation.
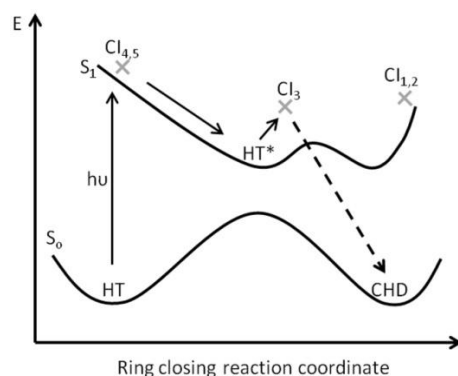
Figure 4. Ring closing reaction labelling scheme. HT, HT*, CHD, CI_i, and hυ are respectively the open-ring ground state, the open-ring excited state intermediate, the closed-ring ground state, the conical intersections, and the photon absorption. Adapted with permission from reference 42. Copyright 2003 American Chemical Society.
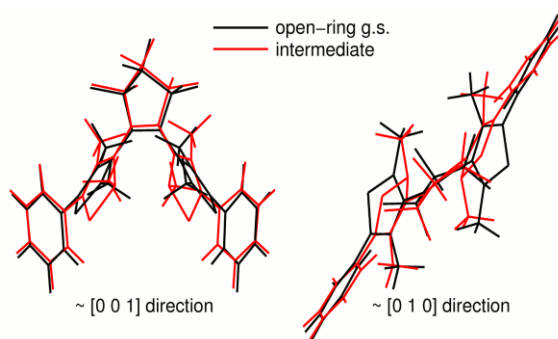
Figure 5. Theoretical model of the open-ring excited state intermediate structure. Front and top view of the optimized geometry of the electronically excited intermediate (red) displayed on top of the optimized ground state open-ring geometry (black).

Overall, the experimental results and quantum mechanical calculations strongly support the reaction mechanism suggested previously[19, 42]. Following photoexcitation and subsequent internal conversion from higher lying states to the S_1 surface, the molecule relaxes from the Franck-Condon geometry to an open-ring minimum on S_1 along the reaction coordinate. The UED measurements confirm that this relaxation involves significant atomic motions, which occur on the sub-ps time scale. The details of a stable intermediate structure are provided by the constructed theoretical model. This relaxation results in the release of a large amount of kinetic energy, which is redistributed among the various vibrational modes of the molecule. Through motions orthogonal to the reaction coordinate, the molecule eventually reaches a conical intersection located in proximity of the S_1 minimum, from which it decays radiationlessly to S_0 and forms the closed-ring photoproduct. The convergence towards the structure of the closed-ring molecule was unambiguously witnessed with UED and it was confirmed to occur with a time constant of approximately 5 ps.

IV. Conclusion

In summary, UED measurements were performed with sub-ps time resolution to investigate the ring closing reaction of a single crystal diarylethene derivative, fully exploiting its cycling capability and thermal irreversibility. The formation of the closed-ring photoproduct was directly observed, in addition to resolving sub-ps structural changes associated with the formation of the reaction intermediate.

Another significant result is the simple observation that a small number of basic modes could fully convert the open-ring structure into the closed-ring one. Here we made use of this finding for generating a pool of molecular structures in order to analyze the UED measurements. However it is more than a mere convenient technicality. Such enormous reduction in dimensionality in barrier crossing regions should be a general observation in complex organic systems. This is what makes chemistry a transferable concept. The exact nature of how low frequency spatially extended modes couple to higher frequency modes to give this reduction is a central issue in chemistry in terms of understanding far from equilibrium fluctuations necessarily involved in chemical processes. The specific motions involved cannot be inferred from static structures alone. The present work paves the way for the use of UED to determine the key atomic motions involved in complex organic systems as part of revealing the general mechanism by which chemistry undergoes dimensional reduction at critical points. The reactions and the scale of the chemical systems that can now be addressed is on par with chemical practice and should be of great utility in helping optimizing desired reaction pathways. As the source technology advances, this approach can ultimately be applied to biological systems as well, where the issues of dimensional reduction and how biological systems coarse grain sample their potential energy surface to transduce chemical potential into functions is a central issue.

References

1.   Sciaini, G.; Miller, R. J. D. Femtosecond Electron Diffraction: Heralding the Era of Atomically Resolved Dynamics. *Reports on Progress in Physics* **2011**, *74* (9), 096101.

2.   Fritz, D. M.; Reis, D. A.; Adams, B.; Akre, R. A.; Arthur, J.; Blome, C.; Bucksbaum, P. H.; Cavalieri, A. L.; Engemann, S.; Fahy, S.; et al. Ultrafast Bond Softening in Bismuth: Mapping a Solid's Interatomic Potential With X-Rays. *Science* **2007**, *315* (5812), 633-636.

3.   Chergui, M.; Zewail, A. H. Electron and X-Ray Methods of Ultrafast Structural Dynamics: Advances and Applications. *Chemphyschem* **2009**, *10* (1), 28-43.

4.   Siwick, B. J.; Dwyer, J. R.; Jordan, R. E.; Miller, R. J. D. An Atomic-Level View of Melting Using Femtosecond Electron Diffraction. *Science* **2003**, *302* (5649), 1382-1385.

5.   Harb, M.; Ernstorfer, R.; Hebeisen, C. T.; Sciaini, G.; Peng, W.; Dartigalongue, T.; Eriksson, M. A.; Lagally, M. G.; Kruglik, S. G.; Miller, R. J. D. Electronically Driven Structure Changes of Si Captured by Femtosecond Electron Diffraction. *Phys Rev Lett* **2008**, *100* (15), 155504.

6.   Sciaini, G.; Harb, M.; Kruglik, S. G.; Payer, T.; Hebeisen, C. T.; zu Heringdorf, F. J.; Yamaguchi, M.; Horn-von Hoegen, M.; Ernstorfer, R.; Miller, R. J. D. Electronic Acceleration of Atomic Motions and Disordering in Bismuth. *Nature* **2009**, *458* (7234), 56-59.

7.   Ernstorfer, R.; Harb, M.; Hebeisen, C. T.; Sciaini, G.; Dartigalongue, T.; Miller, R. J. D. The Formation of Warm Dense Matter: Experimental Evidence for Electronic Bond Hardening in Gold. *Science* **2009**, *323* (5917), 1033-1037.

8.   Eichberger, M.; Schafer, H.; Krumova, M.; Beyer, M.; Demsar, J.; Berger, H.; Moriena, G.; Sciaini, G.; Miller, R. J. D. Snapshots of Cooperative Atomic Motions in the Optical Suppression of Charge Density Waves. *Nature* **2010**, *468* (7325), 799-802.

9.   Erasmus, N.; Eichberger, M.; Haupt, K.; Boshoff, I.; Kassier, G.; Birmurske, R.; Berger, H.; Demsar, J.; Schwoerer, H. Ultrafast Dynamics of Charge Density Waves in 4H(b)-TaSe2 Probed by Femtosecond Electron Diffraction. *Phys Rev Lett* **2012**, *109* (16), 167402.

10.   Han, T.-R. T.; Tao, Z.; Mahanti, S. D.; Chang, K.; Ruan, C.-Y.; Malliakas, C. D.; Kanatzidis, M. G. Structural Dynamics of Two-Dimensional Charge-Density Waves in CeTe_{3} Investigated by Ultrafast Electron Crystallography. *Physical Review B* **2012**, *86* (7), 075145.

11.   Techert, S.; Schotte, F.; Wulff, M. Picosecond X-Ray Diffraction Probed Transient Structural Changes in Organic Solids. *Phys Rev Lett* **2001**, *86* (10), 2030-2033.

12.   Collet, E.; Lemee-Cailleau, M. H.; Buron-Le Cointe, M.; Cailleau, H.; Wulff, M.; Luty, T.; Koshihara, S. Y.; Meyer, M.; Toupet, L.; Rabiller, P.; et al. Laser-Induced Ferroelectric Structural Order in an Organic Charge-Transfer Crystal. *Science* **2003**, *300* (5619), 612-615.

13.   Schotte, F.; Lim, M.; Jackson, T. A.; Smirnov, A. V.; Soman, J.; Olson, J. S.; Phillips, G. N., Jr.; Wulff, M.; Anfinrud, P. A. Watching a Protein as it Functions with 150-ps Time-Resolved X-Ray Crystallography. *Science* **2003**, *300* (5627), 1944-1947.

14.   Hallmann, J.; Morgenroth, W.; Paulmann, C.; Davaasambuu, J.; Kong, Q.; Wulff, M.; Techert, S. Time-resolved X-ray Diffraction of the Photochromic Alpha-Styrylpyrylium Trifluoromethanesulfonate Crystal Films Reveals Ultrafast Structural Switching. *J Am Chem Soc* **2009**, *131* (41), 15018-15025.

15.   Gao, M.; Lu, C.; Jean-Ruel, H.; Liu, L. C.; Marx, A.; Onda, K.; Koshihara, S. Y.; Nakano, Y.; Shao, X.; Hiramatsu, T.; et al. Mapping Molecular Motions Leading to Charge Delocalization with Ultrabright Electrons. *Nature* **2013**, *496* (7445), 343-346.

16.   Dudek, R. C.; Weber, P. M. Ultrafast Diffraction Imaging of the Electrocyclic Ring-Opening Reaction of 1,3-Cyclohexadiene. *The Journal of Physical Chemistry A* **2001**, *105* (17), 4167-4171.

17.   Ihee, H.; Lobastov, V. A.; Gomez, U. M.; Goodson, B. M.; Srinivasan, R.; Ruan, C.-Y.; Zewail, A. H. Direct Imaging of Transient Molecular Structures with Ultrafast Diffraction. *Science* **2001**, *291* (5503), 458-462.

18.   Srinivasan, R.; Feenstra, J. S.; Park, S. T.; Xu, S.; Zewail, A. H. Dark Structures in Molecular Radiationless Transitions Determined by Ultrafast Diffraction. *Science* **2005**, *307* (5709), 558-563.

19.   Jean-Ruel, H.; Cooney, R. R.; Gao, M.; Lu, C.; Kochman, M. A.; Morrison, C. A.; Miller, R. J. D. Femtosecond Dynamics of the Ring Closing Process of Diarylethene: a Case Study of Electrocyclic Reactions in Photochromic Single Crystals. *J Phys Chem A* **2011**, *115* (45), 13158-13168.

20.   Poulin, P. R.; Nelson, K. A. Irreversible Organic Crystalline Chemistry Monitored in Real Time. *Science* **2006**, *313* (5794), 1756-60.

21.   Irie, M. Diarylethenes for Memories and Switches. *Chem Rev* **2000**, *100* (5), 1685-1716.

22.   Tian, H.; Yang, S. Recent Progresses on Diarylethene Based Photochromic Switches. *Chem Soc Rev* **2004**, *33* (2), 85-97.

23.   Irie, M.; Kobatake, S.; Horichi, M. Reversible Surface Morphology Changes of a Photochromic Diarylethene Single Crystal by Photoirradiation. *Science* **2001**, *291* (5509), 1769-1772.

24.   Kobatake, S.; Takami, S.; Muto, H.; Ishikawa, T.; Irie, M. Rapid and Reversible Shape Changes of Molecular Crystals on Photoirradiation. *Nature* **2007**, *446* (7137), 778-781.

25.   Morimoto, M.; Irie, M. A Diarylethene Cocrystal that Converts Light into Mechanical Work. *J Am Chem Soc* **2010**, *132* (40), 14172-14178.

26.   Miyasaka, H.; Araki, S.; Tabata, A.; Nobuto, T.; Malaga, N.; Irie, M. Picosecond Laser Photolysis Studies on Photochromic Reactions of 1,2-Bis(2,4,5-Trimethyl-3-Thienyl)Maleic Anhydride in Solutions. *Chemical Physics Letters* **1991**, *230* (3), 249-254.

27.   Miyasaka, H.; Nobuto, T.; Itaya, A.; Tamai, N.; Irie, M. Picosecond Laser Photolysis Studies on a Photochromic Dithienylethene in Solution and in Crystalline Phases. *Chemical Physics Letters* **1997**, *269* (3–4), 281-285.

28.   Owrutsky, J. C.; Nelson, H. H.; Baronavski, A. P.; Kim, O. K.; Tsivgoulis, G. M.; Gilat, S. L.; Lehn, J. M. Optical Properties and Dynamics of a Photochromic Bisthienylethene in Solution and in a Polymer Film. *Chemical Physics Letters* **1998**, *293* (5–6), 555-563.

29.   Tamai, N.; Saika, T.; Shimidzu, T.; Irie, M. Femtosecond Dynamics of a Thiophene Oligomer with a Photoswitch by Transient Absorption Spectroscopy. *The Journal of Physical Chemistry* **1996**, *100* (12), 4689-4692.

30.   Ern, J.; Bens, A. T.; Martin, H. D.; Mukamel, S.; Tretiak, S.; Tsyganenko, K.; Kuldova, K.; Trommsdorff, H. P.; Kryschi, C. Reaction Dynamics of a Photochromic Fluorescing Dithienylethene. *The Journal of Physical Chemistry A* **2001**, *105* (10), 1741-1749.

31.   Ern, J.; Bens, A. T.; Martin, H.-D.; Kuldova, K.; Trommsdorff, H. P.; Kryschi, C. Ring-Opening and -Closure Reaction Dynamics of a Photochromic Dithienylethene Derivative. *The Journal of Physical Chemistry A* **2002**, *106* (9), 1654-1660.

32.   Hania, P. R.; Telesca, R.; Lucas, L. N.; Pugzlys, A.; van Esch, J.; Feringa, B. L.; Snijders, J. G.; Duppen, K. An Optical and Theoretical Investigation of the Ultrafast Dynamics of a Bisthienylethene-Based Photochromic Switch. *The Journal of Physical Chemistry A* **2002**, *106* (37), 8498-8507.

33.   Bertarelli, C.; Gallazzi, M. C.; Stellacci, F.; Zerbi, G.; Stagira, S.; Nisoli, M.; De Silvestri, S. Ultrafast Photoinduced Ring-Closure Dynamics of a Diarylethene Polymer. *Chemical Physics Letters* **2002**, *359* (3–4), 278-282.

34.   Hania, P. R.; Pugzlys, A.; Lucas, L. N.; de Jong, J. J. D.; Feringa, B. L.; van Esch, J. H.; Jonkman, H. T.; Duppen, K. Ring Closure Dynamics of BTE-Based Photochromic Switches: Perfluoro- versus Perhydrocyclopentene Derivatives. *The Journal of Physical Chemistry A* **2005**, *109* (42), 9437-9442.

35.   Miyasaka, H.; Nobuto, T.; Murakami, M.; Itaya, A.; Tamai, N.; Irie, M. Solvent Viscosity Effects on Photochromic Reactions of a Diarylethene Derivative As Revealed by Picosecond Laser Spectroscopy. *The Journal of Physical Chemistry A* **2002**, *106* (35), 8096-8102.

36.   Okabe, C.; Nakabayashi, T.; Nishi, N.; Fukaminato, T.; Kawai, T.; Irie, M.; Sekiya, H. Picosecond Time-Resolved Stokes and Anti-Stokes Raman Studies on the Photochromic Reactions of Diarylethene Derivatives. *The Journal of Physical Chemistry A* **2003**, *107* (28), 5384-5390.

37.   Shim, S.; Eom, I.; Joo, T.; Kim, E.; Kim, K. S. Ring Closure Reaction Dynamics of Diarylethene Derivatives in Solution. *The Journal of Physical Chemistry A* **2007**, *111* (37), 8910-8917.

38.   Tani, K.; Ishibashi, Y.; Miyasaka, H.; Kobatake, S.; Irie, M. Dynamics of Cyclization, Cycloreversion, and Multiphoton-Gated Reaction of a Photochromic Diarylethene Derivative in Crystalline Phase. *The Journal of Physical Chemistry C* **2008**, *112* (30), 11150-11157.

39.   Uchida, K.; Takata, A.; Ryo, S.-i.; Saito, M.; Murakami, M.; Ishibashi, Y.; Miyasaka, H.; Irie, M. Picosecond Laser Photolysis Studies on a Photochromic Oxidation Polymer Film Consisting of Diarylethene Molecules. *Journal of Materials Chemistry* **2005**, *15* (21), 2128-2133.

40.   Ern, J.; Bens, A. T.; Martin, H. D.; Mukamel, S.; Schmid, D.; Tretiak, S.; Tsiper, E.; Kryschi, C. Reaction Dynamics of Photochromic Dithienylethene Derivatives. *Chemical Physics* **1999**, *246* (1–3), 115-125.

41.   Asano, Y.; Murakami, A.; Kobayashi, T.; Goldberg, A.; Guillaumont, D.; Yabushita, S.; Irie, M.; Nakamura, S. Theoretical Study on the Photochromic Cycloreversion Reactions of Dithienylethenes; on the Role of the Conical Intersections. *J Am Chem Soc* **2004**, *126* (38), 12112-12120.

42.   Boggio-Pasqua, M.; Ravaglia, M.; Bearpark, M. J.; Garavelli, M.; Robb, M. A. Can Diarylethene Photochromism Be Explained by a Reaction Path Alone? A CASSCF Study with Model MMVB Dynamics. *The Journal of Physical Chemistry A* **2003**, *107* (50), 11139-11152.

43.   Gao, M.; Jean-Ruel, H.; Cooney, R. R.; Stampe, J.; de Jong, M.; Harb, M.; Sciaini, G.; Moriena, G.; Miller, R. J. D. Full Characterization of RF Compressed Femtosecond Electron Pulses Using Ponderomotive Scattering. *Opt Express* **2012**, *20* (11), 12048-12058.

44.   Dwyer, J. R.; Hebeisen, C. T.; Ernstorfer, R.; Harb, M.; Deyirmenjian, V. B.; Jordan, R. E.; Miller, R. J. D. Femtosecond Electron Diffraction: 'Making the Molecular Movie'. *Philos Trans A Math Phys Eng Sci* **2006**, *364* (1840), 741-778.

45.   Coppens, P.; Vorontsov, II; Graber, T.; Gembicky, M.; Kovalevsky, A. Y. The Structure of Short-Lived Excited States of Molecular Complexes by Time-Resolved X-Ray Diffraction. *Acta Crystallogr A* **2005**, *61* (2), 162-172.

46.   Vorontsov, II; Coppens, P. On the Refinement of Time-Resolved Diffraction Data: Comparison of the Random-Distribution and Cluster-Formation Models and Analysis of the Light-Induced Increase in the Atomic Displacement Parameters. *J Synchrotron Radiat* **2005**, *12* (4), 488-493.

47.   Kochman, M. A.; Morrison, C. A. Hybrid QM/QM Simulations of Excited-State Intramolecular Proton Transfer in the Molecular Crystal 7-(2-Pyridyl)-indole. *Journal of Chemical Theory and Computation* **2013**, *9* (2), 1182-1192.

48.   Perdew, J. P.; Burke, K.; Ernzerhof, M. Generalized Gradient Approximation Made Simple. *Phys Rev Lett* **1996**, *77* (18), 3865-3868.

49.   Clark, S. J.; Segall, M. D.; Pickard, C. J.; Hasnip, P. J.; Probert, M. I. J.; Refson, K.; Payne, M. C. First Principles Methods Using CASTEP. *Zeitschrift für Kristallographie - Crystalline Materials* **2005**, *220* (5-6-2005), 567-570.

50.   *Materials Studio CASTEP Online Help. H_00PBE.usp uses one valence electron (s state), C_00PBE.usp uses four valence electrons (s and p state), and N_00PBE.usp uses five valence electrons (s and p state).*

51.   Grimme, S. Semiempirical GGA-Type Density Functional Constructed with a Long-Range Dispersion Correction. *J Comput Chem* **2006**, *27* (15), 1787-1799.

52.   Frisch, M. J.; Trucks, G. W.; Schlegel, H. B.; Scuseria, G. E.; Robb, M. A.; Cheeseman, J. R.; Scalmani, G.; Barone, V.; Mennucci, B.; Petersson, G. A.; et al. *Gaussian 09, Revision B.01* **2009**.

53.   Harb, M.; Peng, W.; Sciaini, G.; Hebeisen, C. T.; Ernstorfer, R.; Eriksson, M. A.; Lagally, M. G.; Kruglik, S. G.; Miller, R. J. D. Excitation of Longitudinal and Transverse Coherent Acoustic Phonons in Nanometer Free-Standing Films of (001) Si. *Physical Review B* **2009**, *79* (9), 094301.